Cancer Research

De novo Lipogenesis Protects Cancer Cells from Free Radicals and Chemotherapeutics by Promoting Membrane Lipid Saturation

Evelien Rysman[1], Koen Brusselmans[1], Katryn Scheys[1], Leen Timmermans[1], Rita Derua[2], Sebastian Munck[3], Paul P. Van Veldhoven[4], David Waltregny[5], Veerle W. Daniëls[1], Jelle Machiels[1], Frank Vanderhoydonc[1], Karine Smans[6], Etienne Waelkens[2], Guido Verhoeven[1], and Johannes V. Swinnen[1]

Abstract

Activation of *de novo* lipogenesis in cancer cells is increasingly recognized as a hallmark of aggressive cancers and has been implicated in the production of membranes for rapid cell proliferation. In the current report, we provide evidence that this activation has a more profound role. Using a mass spectrometry–based phospholipid analysis approach, we show that clinical tumor tissues that display the lipogenic phenotype show an increase in the degree of lipid saturation compared with nonlipogenic tumors. Reversal of the lipogenic switch in cancer cells by treatment with the lipogenesis inhibitor soraphen A or by targeting lipogenic enzymes with small interfering RNA leads to a marked decrease in saturated and mono-unsaturated phospholipid species and increases the relative degree of polyunsaturation. Because polyunsaturated acyl chains are more susceptible to peroxidation, inhibition of lipogenesis increases the levels of peroxidation end products and renders cells more susceptible to oxidative stress–induced cell death. As saturated lipids pack more densely, modulation of lipogenesis also alters lateral and transversal membrane dynamics as revealed by diffusion of membrane-targeted green fluorescent protein and by the uptake and response to doxorubicin. These data show that shifting lipid acquisition from lipid uptake toward *de novo* lipogenesis dramatically changes membrane properties and protects cells from both endogenous and exogenous insults. These findings provide important new insights into the role of *de novo* lipogenesis in cancer cells, and they provide a rationale for the use of lipogenesis inhibitors as antineoplastic agents and as chemotherapeutic sensitizers. *Cancer Res; 70(20); 8117–26. ©2010 AACR.*

Introduction

Development and progression of cancer are frequently associated with increased *de novo* production of fatty acids in tumor cells. Activation of *de novo* lipogenesis correlates with a poorer prognosis and shorter disease-free survival for many tumor types (1–4). This metabolic change occurs as a result of common oncogenic insults and is mediated by the activation of multiple lipogenic enzymes. These enzymes are affected at all levels of regulation including transcription, translation, protein stabilization, and protein phosphorylation. Increased lipid production has been linked to an increased need for membranes during rapid cell proliferation, and is considered to be part of a more general metabolic transformation that provides cancer cells with more autonomy in terms of their supply of building blocks for growth (5). In support of this hypothesis, blockade of lipogenesis by chemical inhibitors or RNA interference (RNAi)–mediated silencing of lipogenic enzymes or their regulators attenuates cell proliferation and ultimately leads to cell death (6–16). In several cancer types, overexpression of lipogenic enzymes is observed very early in cancer development and is independent of the proliferative status of the individual cells (17, 18). This suggests that the role of tumor-associated lipogenesis may extend beyond bulk membrane biosynthesis to meet the needs of rapid cell proliferation. Activation of growth factor signaling and protection from cell death are just a few of the emerging novel roles of this pathway (19–22).

In this study, we investigated the most direct effects of lipogenesis, specifically the changes in the lipid composition

Authors' Affiliations: [1]Laboratory for Experimental Medicine and Endocrinology, [2]Division of Biochemistry, [3]Light Microscopy and Imaging Network (LiMoNe) VIB, Department of Molecular and Developmental Genetics, and [4]Laboratory of Lipid Biochemistry and Protein Interactions, K.U. Leuven, Leuven, Belgium; [5]Department of Urology and GIGA Cancer Center, University Hospital of Liège, Liege, Belgium; and [6]Ortho Biotech Oncology Research and Development, Beerse, Belgium

Note: Supplementary data for this article are available at Cancer Research Online (http://cancerres.aacrjournals.org/).

E. Rysman, K. Brusselmans, K. Scheys, L. Timmermans, and R. Derua contributed equally to this work.

Corresponding Author: Johannes V. Swinnen, Laboratory for Experimental Medicine and Endocrinology, K.U. Leuven, Gasthuisberg, O&N 1, Herestraat 49 bus 902, 3000 Leuven, Belgium. Phone: 32-16-330533; Fax: 32-16-345934; E-mail: johan.swinnen@med.kuleuven.be.

doi: 10.1158/0008-5472.CAN-09-3871

of cancer cells, and assessed the consequences of these alterations on cancer cell biology. Our findings suggest that tumor-associated lipogenesis protects cancer cells from carcinogenic- and therapeutic-associated insults by promoting membrane lipid saturation. They also provide a rationale for the use of lipogenesis inhibitors as chemotherapeutic sensitizers.

Materials and Methods

Cell culture and treatments

LNCaP, 22Rv1, PC-3, Du145, BT474, and HCT116 cells were obtained from the American Type Culture Collection (between 2008 and 2010) and authenticated by checking morphology and by karyotyping in December 2009. Cells were cultured in RPMI 1640, DMEM/F-12, or McCoy's 5A medium supplemented with 10% FCS (Invitrogen). Palmitic, linoleic, and linolenic acid (Sigma) were complexed to fatty acid–free bovine serum albumin (Invitrogen) as described (8). Soraphen A was kindly provided by Drs. Klaus Gerth and Rolf Jansen (Helmholtz-Zentrum für Infektionsforschung, Braunschweig, Germany; refs. 23, 24). Doxorubicin and verapamil were obtained from Sigma. Small interfering RNAs (siRNA) targeting fatty acid synthase (FASN) and acetyl-CoA carboxylase-α (ACC) were obtained from Ambion. Multiple siRNA sets were tested. Those with the least off-target effects as judged by microarray analysis (data not shown) were selected for subsequent experiments (s883 and s5030). Silencer Select Negative Control #1 siRNA from Ambion was used as control. Cells were reverse transfected with siRNAs (50 nmol/L) using Lipofectamine RNAiMAX (Invitrogen).

Clinical tissue specimens

Fresh, snap-frozen prostate cancer tissues and matching normal samples were obtained from patients who had undergone a radical retropubic prostatectomy for localized prostatic carcinoma. Harvesting of the tissue samples was performed as previously described (25). The normal and tumor tissues were identified by histologic analysis of areas adjacent to the tissue that was used for lipid and Western blotting analysis. The use of clinical samples was approved by the Local Commission for Medical Ethics and Clinical Studies at the University of Liège.

[2-^{14}C]acetate incorporation assay and TLC analysis

2-^{14}C–labeled acetate (57 mCi/mmol; 2 μCi/dish; Amersham International) was added to the culture medium. Lipids were extracted according to a modified Bligh-Dyer method and analyzed by TLC analysis as described (9).

Quantification of total cellular phospholipids, triglycerides, and cholesterol

Phospholipids, triglycerides, and cholesterol were quantitated as described (26–28).

Gas chromatographic analysis of fatty acyl chains

Aliquots of Bligh-Dyer lipid extracts (9) were supplemented with tricosanoic acid as internal standard, subjected to acidic methanolysis, and analyzed by gas chromatography–mass spectrometry (Trace GC-MS, Thermo Finnigan) using a Supercap 5HT column (15 m × 0.25 mm; 0.10 μm; Alltech). Total ion current signals, obtained in EI$^+$ mode, were related to the internal standard signal and converted to nmol fatty acid using experimentally obtained relative response factors.

Analysis of intact phospholipid species by electrospray ionization tandem mass spectrometry

Tissue or cells were homogenized in 1 N HCl/CH_3OH (1:8, v/v). $CHCl_3$, 200 μg/mL of the antioxidant 2,6-di-*tert*-butyl-4-methylphenol (Sigma; ref. 29), and lipid standards were added. The organic fractions were evaporated and reconstituted in $CH_3OH/CHCl_3/NH_4OH$ (90:10:1.25, v/v/v). Phospholipids were analyzed by electrospray ionization tandem mass spectrometry (ESI-MS/MS) on a hybrid quadrupole linear ion trap mass spectrometer (4000 QTRAP system, Applied Biosystems) equipped with a robotic nanoflow/ion source (Advion Biosciences). The collision energy was varied as follows: prec 184, 50 eV; nl 141, 35 eV; nl 87, −40 eV; prec 241, −55 eV. The system was operated in the multiple reaction monitoring (MRM) mode for quantification of individual species. Typically, a 3-minute period of signal averaging was used for each spectrum. Data were corrected for ^{13}C isotope effects if the contribution was >10%. Corrected data were presented as heat maps using the HeatMap Builder software (Clifton Watt, Stanford University).

Lipid peroxidation product assay

Equal amounts of cells were scraped in ice-cold PBS. After sonication, 3,000 × *g* supernatants were analyzed using a commercial lipid peroxidation assay kit (Oxford Biomedical Research).

Immunoblotting analysis

Equal amounts of protein were loaded onto precast gels (NuPAGE, Invitrogen), transferred to nitrocellulose membranes, and incubated with antibodies against FASN (30), ACC (Cell Signaling Technology), α-tubulin (Cell Signaling Technology), and β-actin (Sigma) as described (8, 9). The ImageMaster 1D software (GE Healthcare) was used for densitometric quantification.

Determination of lateral membrane dynamics by fluorescence recovery after photobleaching and fluorescence diffusion after photoactivation

Cells, grown on Lab-Tek II chambered cover glass (Nunc), were transfected with pAcGFP1-F (Clontech) for FRAP (fluorescence recovery after photobleaching) or with PA-GFP-F (farnesylated photoactivatable form of GFP; ref. 31) for fluorescence diffusion on photoactivation using an Olympus FluoView FV1000 confocal microscope (Olympus America, Inc.) and a Bio-Rad Radiance 2100 confocal system, respectively (31–33). A 405-nm laser diode was used for bleaching (10 seconds at 50 mW) and activation. Full-frame images (512 × 512 pixels) were recorded using a 488-nm argon laser and a 500- to 600-nm band-pass emission filter. Changes in fluorescence were calculated using the FluoView FV1000 software (Olympus).

Determination of flip-flop rate and doxorubicin accumulation

To measure the flip-flop rate of doxorubicin, cells were treated with 10 μmol/L 7-nitrobenzo-2-oxa-1,3-diazole phosphatidylethanolamine (NBD-PE; Invitrogen), exposed to doxorubicin, and monitored in a fluorimeter (excitation, 450 nm; emission, 510 nm) at 37°C. The difference between the NBD fluorescence 2 seconds after the addition of doxorubicin and the NBD fluorescence 4 minutes later was used as the measurement for the relative flip-flop rate of doxorubicin (34). To measure doxorubicin accumulation, the cells were analyzed using a fluorescence microscope (515-nm long-pass emission filter) 30 minutes after addition of doxorubicin (10 μmol/L) or fluorimetrically (excitation, 490 nm; emission, 580 nm).

Cell death assay

At the indicated time after compound exposure, the adherent and floating cells were collected and combined. The viable and dead cells were counted using the trypan blue dye exclusion assay (9). Synergism was determined using the combination index (CI) method (35).

Statistical analysis

The results were analyzed by a Student's *t* test or by one-way ANOVA using a Tukey multiple comparison test. *P* values of <0.05 were considered to be statistically significant. All data presented represent means ± SE, as indicated in the figure legends.

Results and Discussion

Reversal of the lipogenic phenotype depletes cancer cells of saturated and mono-unsaturated acyl chains and causes a shift toward polyunsaturation

To study the effect of tumor-associated lipogenesis on cellular lipid composition, we treated LNCaP prostate cancer cells, which have a high lipogenic activity, with soraphen A (further referred to as soraphen). Soraphen is a highly potent inhibitor of ACC (23, 24, 36) and is an ideal tool to reverse the lipogenic phenotype in cancer cells (12). Consistent with previous studies (12), soraphen treatment decreased the incorporation of ^{14}C- from 2-^{14}C–labeled acetate into phospholipids and triglycerides by 7- and 13-fold, respectively (Fig. 1A) and led to a 1.7- and 4.2-fold reduction of the total phospholipid and triglyceride levels, respectively (Fig. 1B). Cholesterol levels remained unaffected.

Because mammalian cells have a limited ability to synthesize polyunsaturated fatty acids *de novo*, as they lack the Δ12 desaturase required to produce fatty acids of the ω3 and ω6 series, we hypothesized that *de novo* lipogenesis would enrich cancer cells mainly with saturated and/or mono-unsaturated acyl chains and that reversal of the lipogenic phenotype would cause a selective reduction in the levels of these latter acyl species. To test this hypothesis, the total cellular lipid extracts were methanolysed, and the generated fatty acyl methyl esters were analyzed by gas chromatography. Soraphen treatment decreased the total levels of palmitoyl (16:0), stearoyl (18:0), and oleoyl (18:1) species by ~2-fold. The levels of polyunsaturated acyl chain species, the precursors of which were obligatorily derived from the medium (containing 10% serum), substantially increased (Fig. 1C). The net result was (*a*) an overall decrease in cellular acyl content, confirming the importance of *de novo* lipogenesis for quantitative lipid supply, and (*b*) a major shift in cellular acyl chain composition toward polyunsaturation; the relative cellular contribution of saturated acyl chains dropped from 38% to 29% and polyunsaturated fatty acids increased from 9% to 20%.

Based on our observation that most of the labeled acyl chains were incorporated into phospholipids in cancer cells (Fig. 1A) and given the importance of phospholipid acyl chain composition in numerous membrane-related functions, we further investigated the effects of soraphen treatment on intact phospholipids by ESI-MS/MS. As shown in Fig. 1D, soraphen treatment substantially decreased phosphatidylcholine (PC) species with zero or one degree of unsaturation (both acyl chains combined) up to 4-fold, whereas species with polyunsaturated chains (more than three unsaturations in both chains combined) increased up to 8-fold, depending on the species. A similar trend toward decreased saturation and increased polyunsaturation was also observed for phosphatidylethanolamine and phosphatidylserine (Supplementary Fig. S1); however, these effects were less pronounced and less general compared with those of PC.

The observed changes in membrane lipid saturation were not unique to LNCaP cells. Similar effects were observed in all lipogenic cancer cell lines tested. These included three other prostate cancer cell lines (22Rv1, PC-3, and Du145), a breast cancer cell line (BT474), and a colorectal cancer cell line (HCT116; Fig. 1D). Changes were most outspoken in LNCaP and in HCT116 cells. Importantly, a similar shift in membrane lipid saturation was seen after siRNA-mediated knockdown of the lipogenic enzymes FASN or ACC (siRNA) instead of treatment with soraphen (Fig. 1E). Effects were somewhat less pronounced than after soraphen treatment, reflecting the less potent inhibition of lipogenesis [2- to 3-fold reduction in the incorporation of ^{14}C- from 2-^{14}C–labeled acetate into lipids (Supplementary Fig. S2) versus an 8-fold reduction after soraphen treatment]. Overall, these data strongly support the hypothesis that the lipogenic phenotype in cancer cells provides cells with saturated and mono-unsaturated acyl chains, which replenishes the cells with membrane components and simultaneously increases the relative degree of saturation of phospholipids, particularly that of PC.

Activation of the lipogenic pathway is associated with increased saturation of phospholipids *in vivo* in human tumor specimens

To assess whether the lipogenic phenotype of cancer cells is associated with an increased saturation of phospholipids *in vivo*, prostate tumor specimens and normal matching control tissues were analyzed for overexpression of FASN by Western blot analysis, and the phospholipid profiles were recorded. Three of the five matched samples (tumor versus

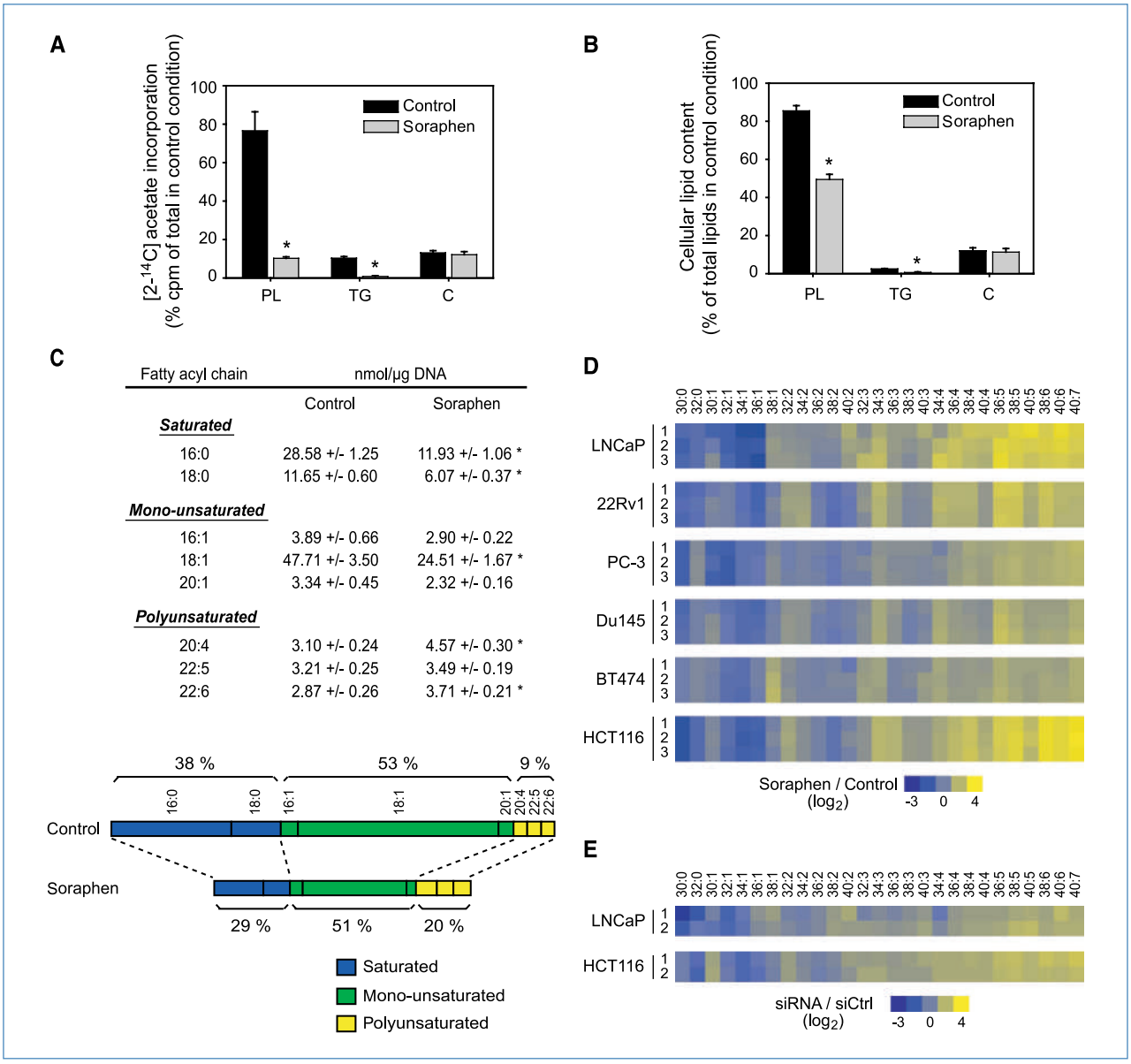

Figure 1. Effect of inhibition of *de novo* lipogenesis on the cellular lipid composition of cancer cells *in vitro*. A, effect of soraphen on lipid synthesis. LNCaP cells were treated with soraphen (100 nmol/L) or vehicle (control) for 24 h. During the last 4 h, 2-[^{14}C]acetate was added. ^{14}C incorporation in phospholipids (PL), triglycerides (TG), and cholesterol (C) was analyzed by TLC. Columns, mean (n = 4); bars, SE. *, $P < 0.05$, significantly different from control. B, effect of soraphen on cellular lipid content of LNCaP cells 72 h after addition of soraphen (100 nmol/L) or vehicle (control; n = 3). C, effect of soraphen treatment on cellular lipid acyl chain composition of LNCaP cells. Lipid extracts as in B were hydrolyzed and analyzed by gas chromatography (n = 3). The scheme represents the contribution of the fatty acyl chains listed relative to their sum (in nmol/µg DNA) in both control and soraphen-treated cells. D, effect of soraphen treatment on intact PC species in different cancer cell lines. Lipid extracts as in B were analyzed by ESI-MS/MS (precursor 184) in the MRM mode. Lipid profiling was performed in three pairs of samples (1–3). The heat maps show the soraphen/control ratio (expressed as $\log_2$) for different PC species. E, effect of RNAi targeting lipogenic genes on intact PC species. LNCaP and HCT116 cells were transfected with 50 nmol/L siRNA targeting FASN or ACC, respectively. Lipid profiling was performed after 72 to 96 h in two pairs of samples (1–2). The heat maps show the siRNA/siCtrl ratio (expressed as $\log_2$) for different PC species.

control) showed a substantial overexpression of FASN in tumor tissue (Fig. 2). Analysis of the phospholipid composition by ESI-MS/MS showed a different profile for PC in the lipogenic tumors compared with the nonlipogenic tumors. The tumors with increased FASN expression showed a consistent increase in saturated and mono-unsaturated acyl chains and a decrease in polyunsaturated species in tumor tissue compared with matching normal tissue (Fig. 2). These data support our findings with the lipogenesis inhibitor soraphen and with the siRNA-mediated knockdown of lipogenic enzymes

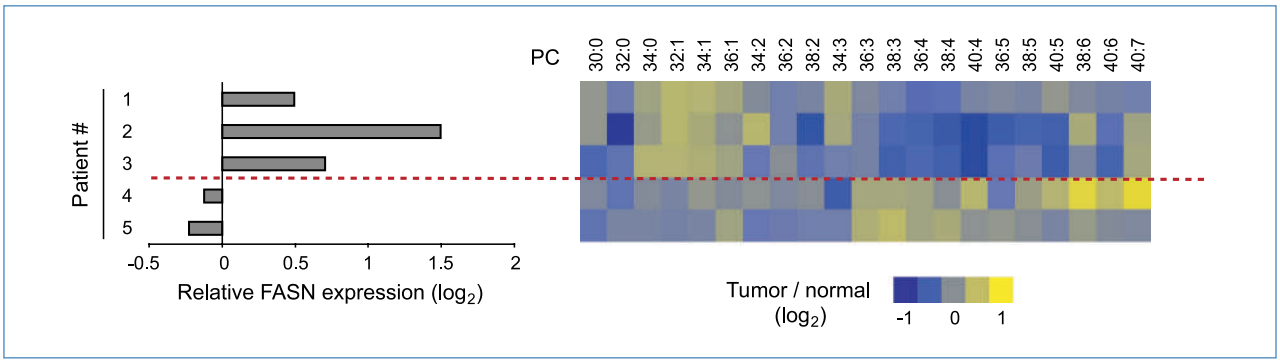

Figure 2. Changes in phospholipid composition in lipogenic and nonlipogenic prostate tumor tissue specimens versus matched normal tissue. Expression of FASN in matched pairs of malignant versus normal prostate tissue specimens was measured by Western blotting analysis, and the expression was normalized to β-actin expression. Values are expressed as a ratio (log_2) of tumor over matching normal tissue. The relative abundances of PC species were recorded by ESI-MS/MS in the MRM mode. The heat map shows the tumor/normal ratio (expressed as log_2) for different PC species.

in cancer cell lines, and they provide *in vivo* evidence that tumor-associated lipogenesis increases the saturation of phospholipids in human tumors.

Modulation of *de novo* fatty acid synthesis in cancer cells affects the susceptibility of cellular membranes to lipid peroxidation

Saturated, mono-unsaturated, and polyunsaturated acyl chains dramatically differ in terms of their structural and physicochemical properties. One of the key differences is their susceptibility to peroxidation. In this process, free radicals extract electrons from lipids in cellular membranes, which leads to the formation of oxidized lipid species. These lipid species have important biological functions and may ultimately degrade into smaller reactive products including malondialdehydes and 4-hydroxyalkenals, which can cause cell damage when expressed at high levels (37–39). As the hydrogens in between double bonds in methylene (CH2) groups are particularly reactive, polyunsaturated acyl chains are much more susceptible to peroxidation. Consistent with our observation that modulation of *de novo* fatty acid synthesis in cancer cells affects the balance between (mono-un) saturated and polyunsaturated acyl chains in the phospholipids of cellular membranes, soraphen treatment significantly increased the levels of lipid peroxidation products (Fig. 3A). Treatment with exogenous H_2O_2, which produces higher levels

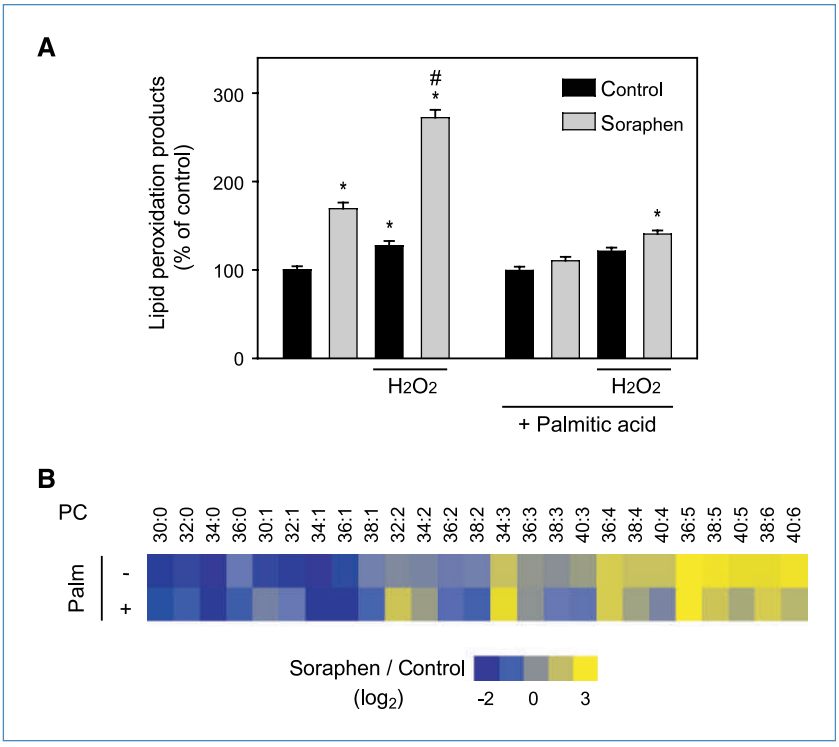

Figure 3. Modulation of lipogenesis affects the susceptibility of cellular membranes to lipid peroxidation. A, effects of soraphen, H_2O_2, and palmitic acid on lipid peroxidation products. LNCaP cells were treated with soraphen (100 nmol/L) or vehicle (control) and with palmitic acid (75 μmol/L) for 72 h. During the last 2 h, the cells were exposed to 200 μmol/L H_2O_2. Equal amounts of cells were analyzed for lipid peroxidation products using a lipid peroxidation assay kit. Columns, mean (n = 4); bars, SE. *, $P < 0.05$, significantly different from control without H_2O_2 exposure; #, $P < 0.05$, significantly different from both treatment with H_2O_2 and soraphen alone. B, effect of palmitic acid on the PC profile. PC species were analyzed by ESI-MS/MS in the MRM mode. The heat map shows the soraphen/control ratio (expressed as log_2) for different PC species.

of free radicals, induced a further increase in peroxidation products. Interestingly, partial replenishment of saturated acyl chains by supplementation of the medium with exogenous palmitic acid (Fig. 3B) largely reversed these changes, supporting the idea that enhanced lipogenesis renders cancer cells less susceptible to lipid peroxidation by limiting the degree of phospholipid polyunsaturation.

De novo lipogenesis determines the sensitivity of cancer cells to oxidative stress–induced cell death

There is growing evidence that oxidized phospholipids and their degradation products play a key role in the induction and mediation of cellular apoptosis (40–43). Therefore, we investigated whether modulation of *de novo* lipogenesis affected the sensitivity of cancer cells to oxidative stress–induced cell death. The native LNCaP cells were fairly resistant to H_2O_2-induced cell death, but pretreatment with soraphen markedly increased their death in response to H_2O_2, as shown by trypan blue staining (Fig. 4A). These effects were counteracted by exogenous palmitic acid. Interestingly, when the medium was supplemented with a mixture of saturated and polyunsaturated fatty acids, the rescue effect was much less pronounced. These data indicate that the increased sensitivity to oxidative stress observed after soraphen treatment is not due to the general decrease in the amount of lipids but rather to the change in lipid (un)saturation. Concordant results were obtained in 22Rv1 cells (Fig. 4A) and in PC-3, BT474, and HCT116 cells (Supplementary Fig. S3). Similarly, siRNA-mediated knockdown of the lipogenic pathway increased the sensitivity to oxidative stress–induced cell death, as illustrated for LNCaP and HCT116 cells (Fig. 4B). Overall, these data support the idea that increased lipogenesis protects cancer cells from oxidative stress–induced cell death by changing the extent of saturation of cellular membranes.

Tumor-associated fatty acid synthesis alters membrane dynamics and affects the uptake and response to common chemotherapeutics

In addition to its effect on lipid peroxidation, modulation of membrane lipid composition is known to have a major effect

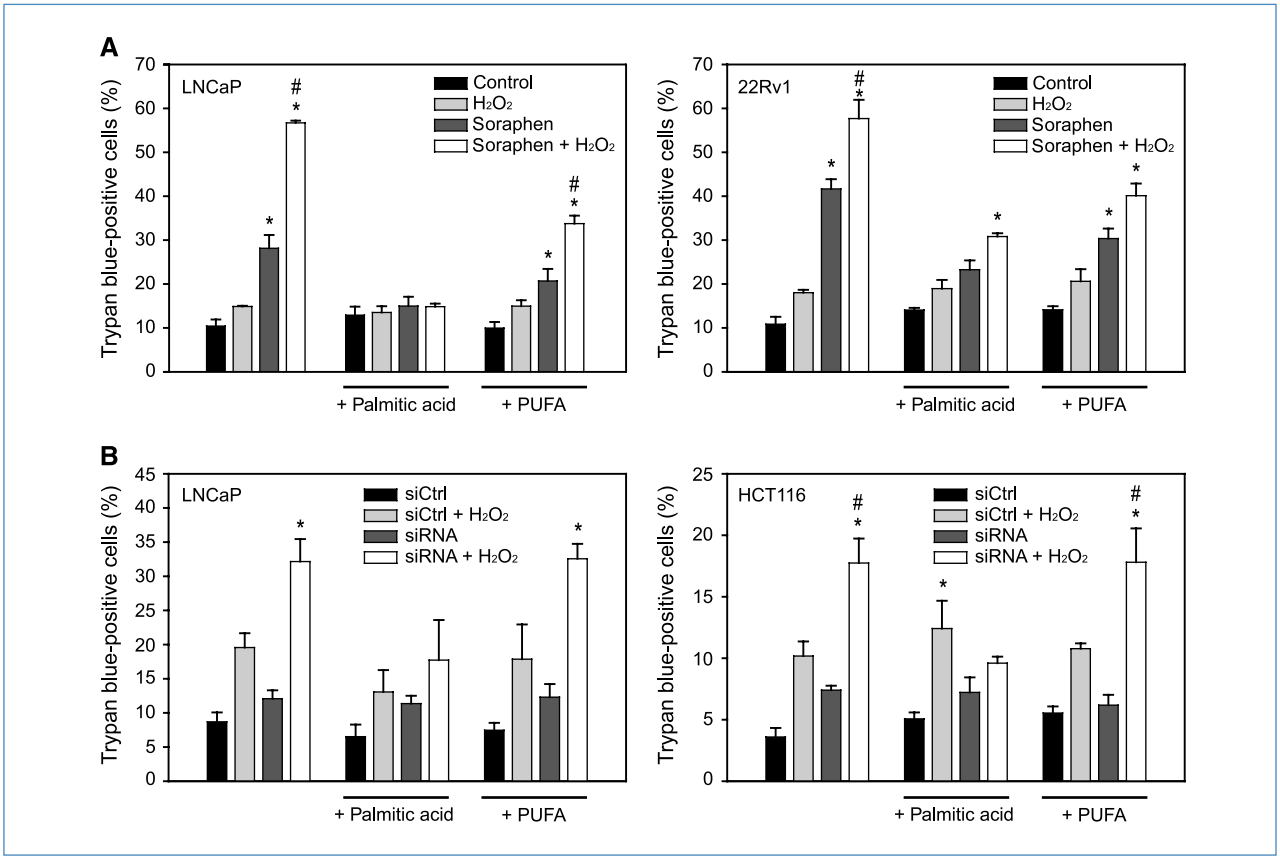

Figure 4. *De novo* lipogenesis in cancer cells determines their sensitivity to oxidative stress–induced cell death. A, LNCaP and 22Rv1 cells were treated with soraphen (100 nmol/L) or vehicle (control) and with palmitic acid (75 μmol/L) or with a mixture of 10% palmitic, 45% linoleic, and 45% linolenic acid (PUFA; 75 μmol/L total) for 72 h. During the last 24 h, cells were exposed to 300 μmol/L H_2O_2. B, LNCaP and HCT116 cells were transfected with 50 nmol/L siRNA targeting FASN or ACC (siRNA), respectively, or with control siRNA (siCtrl). Cells were treated with palmitic acid (75 μmol/L) or PUFA (75 μmol/L total) for 72 h. During the last 24 h, cells were exposed to 300 or 400 μmol/L H_2O_2, respectively. Cells were collected and stained with trypan blue to assess cell viability. Columns, mean ($n = 3$); bars, SE. *, $P < 0.05$, significantly different from control/siCtrl; #, $P < 0.05$, significantly different from both treatment with H_2O_2 and soraphen/siRNA alone.

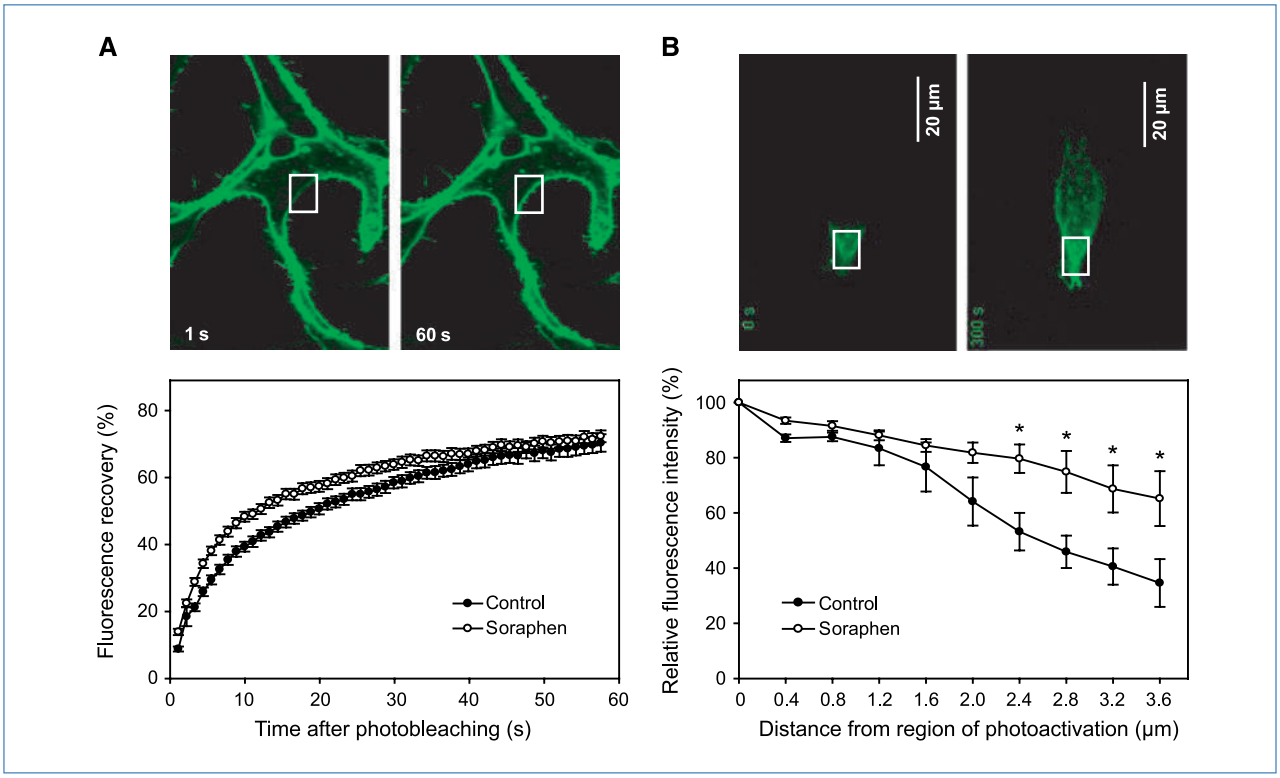

Figure 5. Modulation of lipogenesis alters membrane dynamics. A, FRAP analysis of the effect of soraphen on the lateral dynamics of farnesylated green fluorescent protein (GFP). LNCaP cells were transfected with a farnesylated GFP construct and treated with soraphen (100 nmol/L) or vehicle (control). After 72 h, the fluorescence was bleached in a specific region (white squares). The fluorescence recovery was analyzed at the indicated time points. Points, mean (n = 41–44); bars, SE. Values from soraphen-treated cells were significantly different from control ($P < 0.05$) from 1 to 43 s after bleaching. B, analysis of lateral dynamics of photoactivatable GFP. LNCaP cells were transfected with a photoactivatable farnesylated GFP construct and treated with soraphen (100 nmol/L) or vehicle (control). After 72 h, the diffusion of fluorescence along the plasma membrane was analyzed after photoactivation of farnesylated GFP in a specific region (white squares). The fluorescence was measured as a function of the distance from this region. Points, mean (n = 4; at time = 4 s); bars, SE. Data are expressed as the % fluorescence intensity compared with the fluorescence intensity in the region of photoactivation at time 0. *, $P < 0.05$, significantly different from control.

on the mobility of membrane components (38, 44). To examine whether modulation of *de novo* fatty acid synthesis in cancer cells exerts similar effects, we investigated the effect of soraphen on both the lateral and transversal mobility of membrane components in LNCaP cells. Lateral mobility refers to the movement of membrane components within the plane of one membrane leaflet, whereas transversal mobility refers to movement from one leaflet to the other. To analyze lateral membrane mobility, we followed the movement of membrane-targeted GFP using two complementary techniques: FRAP and fluorescence diffusion after photoactivation. To perform FRAP, we transiently transfected LNCaP cells with the plasmid pAcGFP1-F that encodes GFP with a farnesylation tag. We bleached the fluorescence in a small area and measured the recovery of fluorescence in this area, which is mediated by neighboring GFP molecules moving into the bleached area. As shown in Fig. 5A, soraphen-treated cells had a faster fluorescence recovery rate compared with control cells. Similar results were obtained with BT474 cells (Supplementary Fig. S4). In the complementary experiment, LNCaP cells were transfected with a plasmid encoding a farnesylated photoactivatable form of GFP (PA-GFP-F). At a fixed time point after photoactivation of GFP in a small spot of the plasma membrane, the fluorescence intensity was measured as a function of the distance from the spot of photoactivation. The slope of the curve for the soraphen-treated cells was less steep than that for the control cells, reflecting a higher diffusion rate (Fig. 5B). Together with the FRAP data, these results indicate that inhibition of fatty acid synthesis increases the lateral mobility of membrane components.

Transversal mobility of membrane components, also referred to as flip-flop, occurs at a low rate unless it is facilitated by specific transporters. However, for certain exogenous compounds including commonly used chemotherapeutics, such as doxorubicin, passive flip-flop is a major mechanism of entry into the cells (34). Because treatment of cells with exogenous polyunsaturated fatty acids is known to promote the uptake of doxorubicin (45), we determined whether inhibition of fatty acid synthesis would promote membrane flip-flop and doxorubicin uptake. The flip-flop of doxorubicin was assessed by monitoring doxorubicin-mediated quenching of NBD-PE, a fluorescently labeled phospholipid that incorporates into

both leaflets of the plasma membrane. After addition of doxorubicin, there was a rapid quenching of NBD fluorescence, which is caused by the association of doxorubicin with phospholipids in the outer leaflet. As doxorubicin translocates to the inner leaflet, further quenching of NBD is observed (34). Monitoring of NBD quenching indicated that soraphen induced a 6-fold increase in the flip-flop rate of doxorubicin (Fig. 6A). These effects were not caused by indirect effects of P-glycoprotein, which pumps hydrophobic molecules such as doxorubicin out of the cell, because similar results were

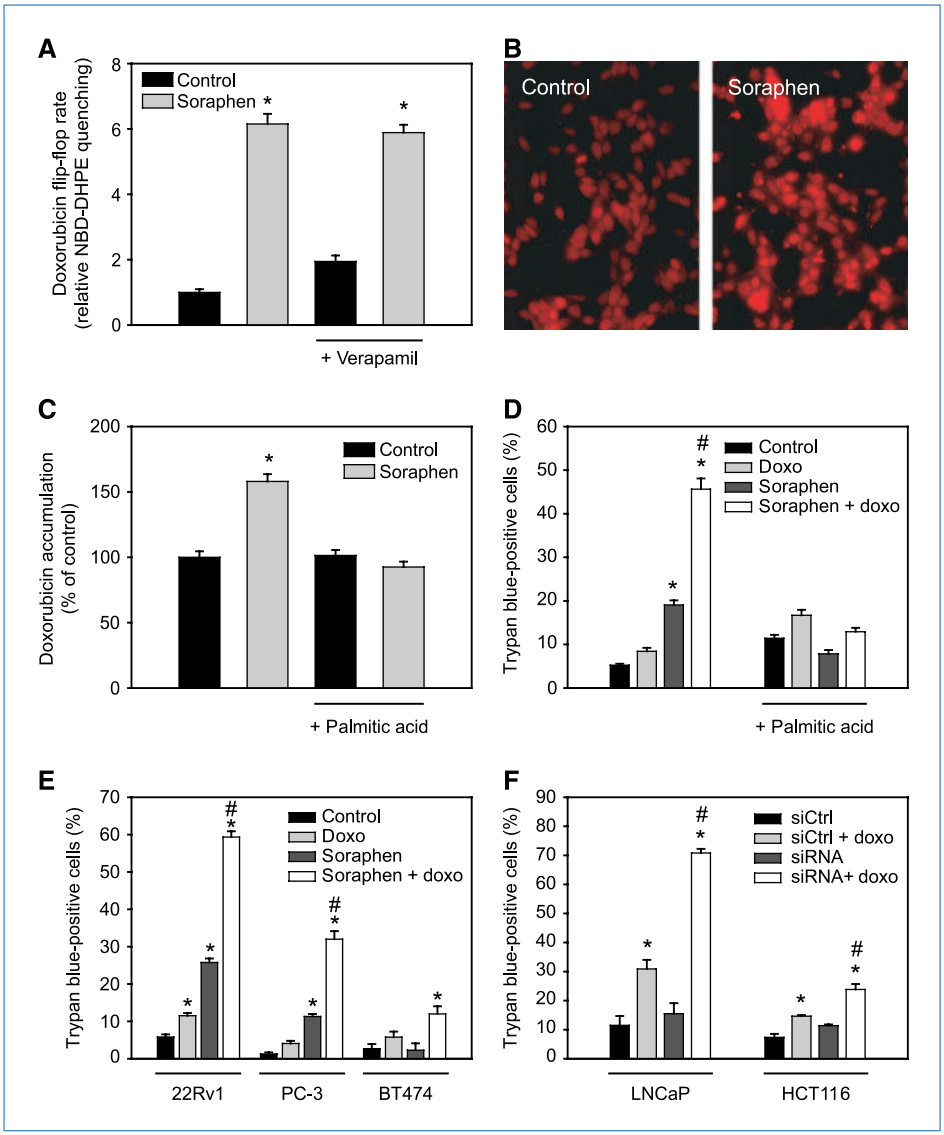

Figure 6. Inhibition of fatty acid synthesis in cancer cells affects the uptake and cytotoxicity of doxorubicin. A, effect of soraphen on the flip-flop rate of doxorubicin. LNCaP cells were cultured with or without soraphen (100 nmol/L) for 72 h. During the last 24 h, NBD-DHPE (10 μmol/L) was added to the cells. An hour before analysis, the cells were treated with vehicle or verapamil (100 μmol/L). Equal amounts of cells were collected, doxorubicin (10 μmol/L) was added, and the NBD fluorescence was continuously monitored to determine the level of quenching by doxorubicin ($n = 4$). B and C, effect of soraphen on doxorubicin accumulation. LNCaP cells were cultured in the presence or absence of soraphen (100 nmol/L) and palmitic acid (75 μmol/L) for 72 h. Doxorubicin (10 μmol/L) was added and, 2 h later, visualized by fluorescence microscopy (B) and quantified by fluorimetry ($n = 4$; C). D, effect of soraphen and palmitic acid on doxorubicin-induced cytotoxicity. LNCaP cells were treated with soraphen and palmitic acid as in C. During the last 24 h, doxorubicin (4 μmol/L) or vehicle was added. The cells were collected and stained with trypan blue to assess the cell viability ($n = 6$–12). E, effect of soraphen on doxorubicin-induced cell death in other cancer cell lines. 22Rv1, PC-3, and BT474 cells were treated with or without 100 nmol/L soraphen for 72 h and with 4 μmol/L doxorubicin or vehicle during the last 24 h ($n = 3$). F, effect of RNAi targeting lipogenic genes on doxorubicin-induced cytotoxicity. LNCaP and HCT116 cells were transfected with 50 nmol/L siRNA targeting FASN or ACC (siRNA), respectively, or with control siRNA (siCtrl). During the last 24 h, cells were exposed to 2 or 4 μmol/L doxorubicin, respectively ($n = 3$). Columns, mean; bars, SE. *, $P < 0.05$, significantly different from control/siCtrl; #, $P < 0.05$, significantly different from both soraphen/siRNA and doxorubicin alone.

obtained in the presence of the P-glycoprotein inhibitor verapamil (Fig. 6A). The increased flip-flop rate was accompanied by a significant increase in the intracellular accumulation of doxorubicin, as assessed by fluorescence microscopy and fluorimetric analysis of cellular extracts and as shown also for 22Rv1 and PC-3 cells (Fig. 6B and C; Supplementary Fig. S5). Addition of exogenous palmitic acid counteracted the effects of soraphen (Fig. 6C). Soraphen treatment markedly sensitized LNCaP cells to the cytotoxic effects of doxorubicin, which was consistent with the increased accumulation of doxorubicin in soraphen-treated cells and their increased susceptibility to cell death. LNCaP cells grown under standard culture conditions were fairly resistant to doxorubicin-induced cell death (8% cell death at 4 μmol/L; Fig. 6D), but pretreatment with soraphen, which alone induced death in up to 20% of the cells, increased the rate of cell death to ~50%. This potent effect was synergistic, as assessed using the CI method (Supplementary Fig. S6; ref. 35). Addition of exogenous palmitic acid counteracted these effects and largely rescued the cells from death (Fig. 6D). Concordant results were obtained with the prostate cancer cell lines 22Rv1 and PC-3 and with the breast cancer cell line BT474 (Fig. 6E). Similarly, knockdown of the lipogenic pathway with siRNA sensitized the cancer cells for doxorubicin-induced cytotoxicity (Fig. 6F). These findings suggest that increased lipogenesis in cancer cells may limit the uptake of chemotherapeutics and, together with the mentioned changes in susceptibility to cell death, may render cancer cells less susceptible to cytotoxic agents. Conversely, these data provide a new rationale for the use of lipogenesis inhibitors to increase the efficacy of chemotherapeutic agents.

Conclusion

The results from this study show that the implications of increased lipogenesis, which frequently accompanies cancer progression, extend beyond its commonly accepted role in providing lipids for rapid cell proliferation, as we provide direct evidence that cancer cells promote saturation of their membranes and modulate their biophysical properties by activating *de novo* lipogenesis. As (mono-un)saturated lipids are less susceptible to lipid peroxidation, this shift may protect cancer cells from lipid peroxidation–mediated cell death. It also alters membrane dynamics and affects the uptake and efficacy of chemotherapeutics. The findings from this study suggest that tumor-associated lipogenesis confers a significant advantage to cancer cells, as it helps them to survive both carcinogenic- and therapeutic-mediated insults. This study also provides a novel strategy for the use of lipogenesis inhibitors for therapeutic intervention, particularly as therapy sensitizers.

Disclosure of Potential Conflicts of Interest

No potential conflicts of interest were disclosed.

Acknowledgments

We thank Drs. Klaus Gerth and Rolf Jansen for soraphen A.

Grant Support

K.U. Leuven grants OT/07/068A and GOA 2008/16; Research Foundation-Flanders grant G.0590.08; "Stichting tegen Kanker"; and Interuniversity Poles of Attraction Programme–Belgian State, Prime Minister's Office, Federal Office for Scientific, Technical and Cultural affairs. E. Rysman, L. Timmermans, K. Scheys, and V.W. Daniëls are research assistants and K. Brusselmans is a postdoctoral fellow of the Research Foundation-Flanders.

The costs of publication of this article were defrayed in part by the payment of page charges. This article must therefore be hereby marked *advertisement* in accordance with 18 U.S.C. Section 1734 solely to indicate this fact.

Received 11/16/2009; revised 06/14/2010; accepted 07/18/2010; published OnlineFirst 09/28/2010.

References

1. Brusselmans K, Swinnen JV. The lipogenic switch in cancer. In: Singh KK, Costello LC, editors. Mitochondria and cancer. New York: Springer; 2009, p. 39–59.
2. Kuhajda FP. Fatty acid synthase and cancer: new application of an old pathway. Cancer Res 2006;66:5977–80.
3. Menendez JA, Lupu R. Fatty acid synthase and the lipogenic phenotype in cancer pathogenesis. Nat Rev Cancer 2007;7:763–77.
4. Swinnen JV, Brusselmans K, Verhoeven G. Increased lipogenesis in cancer cells: new players, novel targets. Curr Opin Clin Nutr Metab Care 2006;9:358–65.
5. DeBerardinis RJ, Lum JJ, Hatzivassiliou G, Thompson CB. The biology of cancer: metabolic reprogramming fuels cell growth and proliferation. Cell Metab 2008;7:11–20.
6. Pizer ES, Jackisch C, Wood FD, Pasternack GR, Davidson NE, Kuhajda FP. Inhibition of fatty acid synthesis induces programmed cell death in human breast cancer cells. Cancer Res 1996;56:2745–7.
7. Kuhajda FP, Jenner K, Wood FD, et al. Fatty acid synthesis: a potential selective target for antineoplastic therapy. Proc Natl Acad Sci U S A 1994;91:6379–83.
8. Brusselmans K, De Schrijver E, Verhoeven G, Swinnen JV. RNA interference-mediated silencing of the acetyl-CoA-carboxylase-α gene induces growth inhibition and apoptosis of prostate cancer cells. Cancer Res 2005;65:6719–25.
9. De Schrijver E, Brusselmans K, Heyns W, Verhoeven G, Swinnen JV. RNA interference-mediated silencing of the fatty acid synthase gene attenuates growth and induces morphological changes and apoptosis of LNCaP prostate cancer cells. Cancer Res 2003;63:3799–804.
10. Kridel SJ, Axelrod F, Rozenkrantz N, Smith JW. Orlistat is a novel inhibitor of fatty acid synthase with antitumor activity. Cancer Res 2004;64:2070–5.
11. Kridel SJ, Lowther WT, Pemble CW. Fatty acid synthase inhibitors: new directions for oncology. Expert Opin Investig Drugs 2007;16:1817–29.
12. Beckers A, Organe S, Timmermans L, et al. Chemical inhibition of acetyl-CoA carboxylase induces growth arrest and cytotoxicity selectively in cancer cells. Cancer Res 2007;67:8180–7.
13. Chajes V, Cambot M, Moreau K, Lenoir GM, Joulin V. Acetyl-CoA carboxylase α is essential to breast cancer cell survival. Cancer Res 2006;66:5287–94.
14. Hatzivassiliou G, Zhao F, Bauer DE, et al. ATP citrate lyase inhibition can suppress tumor cell growth. Cancer Cell 2005;8:311–21.
15. Donnelly C, Olsen AM, Lewis LD, Eisenberg BL, Eastman A, Kinlaw WB. Conjugated linoleic acid (CLA) inhibits expression of the Spot 14 (THRSP) and fatty acid synthase genes and impairs the growth of human breast cancer and liposarcoma cells. Nutr Cancer 2009;61:114–22.

16. Kinlaw WB, Quinn JL, Wells WA, Roser-Jones C, Moncur JT. Spot 14: a marker of aggressive breast cancer and a potential therapeutic target. Endocrinology 2006;147:4048–55.
17. Piyathilake CJ, Frost AR, Manne U, et al. The expression of fatty acid synthase (FASE) is an early event in the development and progression of squamous cell carcinoma of the lung. Hum Pathol 2000;31: 1068–73.
18. Milgraum LZ, Witters LA, Pasternack GR, Kuhajda FP. Enzymes of the fatty acid synthesis pathway are highly expressed in *in situ* breast carcinoma. Clin Cancer Res 1997;3:2115–20.
19. Little JL, Wheeler FB, Fels DR, Koumenis C, Kridel SJ. Inhibition of fatty acid synthase induces endoplasmic reticulum stress in tumor cells. Cancer Res 2007;67:1262–9.
20. Fiorentino M, Zadra G, Palescandolo E, et al. Overexpression of fatty acid synthase is associated with palmitoylation of Wnt1 and cytoplasmic stabilization of β-catenin in prostate cancer. Lab Invest 2008;88:1340–8.
21. Migita T, Ruiz S, Fornari A, et al. Fatty acid synthase: a metabolic enzyme and candidate oncogene in prostate cancer. J Natl Cancer Inst 2009;101:519–32.
22. Vazquez-Martin A, Colomer R, Brunet J, Lupu R, Menendez JA. Overexpression of fatty acid synthase gene activates HER1/HER2 tyrosine kinase receptors in human breast epithelial cells. Cell Prolif 2008;41:59–85.
23. Bedorf N, Schomburg D, Gerth K, Reichenbach H, Hofle G. Isolation and structure elucidation of soraphen A1, a novel antifungal macrolide from *Sorangium cellulosum*. Liebigs Ann Chem 1993:1017–21.
24. Gerth K, Bedorf N, Irschik H, Hofle G, Reichenbach H. The soraphens: a family of novel antifungal compounds from *Sorangium cellulosum* (Myxobacteria). I. Soraphen A1α: fermentation, isolation, biological properties. J Antibiot (Tokyo) 1994;47:23–31.
25. Waltregny D, Alami Y, Clausse N, de Leval J, Castronovo V. Overexpression of the homeobox gene HOXC8 in human prostate cancer correlates with loss of tumor differentiation. Prostate 2002;50: 162–9.
26. Van Veldhoven PP, Bell RM. Effect of harvesting methods, growth conditions and growth phase on diacylglycerol levels in cultured human adherent cells. Biochim Biophys Acta 1988;959:185–96.
27. Van Veldhoven PP, Swinnen JV, Esquenet M, Verhoeven G. Lipase-based quantitation of triacylglycerols in cellular lipid extracts: requirement for presence of detergent and prior separation by thin-layer chromatography. Lipids 1997;32:1297–300.
28. Van Veldhoven PP, Meyhi E, Mannaerts GP. Enzymatic quantitation of cholesterol esters in lipid extracts. Anal Biochem 1998;258:152–5.
29. Milne S, Ivanova P, Forrester J, Alex BH. Lipidomics: an analysis of cellular lipids by ESI-MS. Methods 2006;39:92–103.
30. Van de Sande T, De Schrijver E, Heyns W, Verhoeven G, Swinnen JV. Role of the phosphatidylinositol 3′-kinase/PTEN/Akt kinase pathway in the overexpression of fatty acid synthase in LNCaP prostate cancer cells. Cancer Res 2002;62:642–6.
31. Patterson GH, Lippincott-Schwartz J. A photoactivatable GFP for selective photolabeling of proteins and cells. Science 2002;297: 1873–7.
32. Sauer H, Putz V, Fischer K, Hescheler J, Wartenberg M. Increased doxorubicin uptake and toxicity in multicellular tumour spheroids treated with DC electrical fields. Br J Cancer 1999;80:1204–13.
33. Runions J, Brach T, Kuhner S, Hawes C. Photoactivation of GFP reveals protein dynamics within the endoplasmic reticulum membrane. J Exp Bot 2006;57:43–50.
34. Regev R, Yeheskely-Hayon D, Katzir H, Eytan GD. Transport of anthracyclines and mitoxantrone across membranes by a flip-flop mechanism. Biochem Pharmacol 2005;70:161–9.
35. Chou TC, Talalay P. Quantitative analysis of dose-effect relationships: the combined effects of multiple drugs or enzyme inhibitors. Adv Enzyme Regul 1984;22:27–55.
36. Shen Y, Volrath SL, Weatherly SC, Elich TD, Tong L. A mechanism for the potent inhibition of eukaryotic acetyl-coenzyme A carboxylase by soraphen A, a macrocyclic polyketide natural product. Mol Cell 2004;16:881–91.
37. Deigner HP, Hermetter A. Oxidized phospholipids: emerging lipid mediators in pathophysiology. Curr Opin Lipidol 2008;19:289–94.
38. Rabinovich AL, Ripatti PO. On the conformational, physical properties and functions of polyunsaturated acyl chains. Biochim Biophys Acta 1991;1085:53–62.
39. Schneider C, Porter NA, Brash AR. Routes to 4-hydroxynonenal: fundamental issues in the mechanisms of lipid peroxidation. J Biol Chem 2008;283:15539–43.
40. West JD, Ji C, Duncan ST, et al. Induction of apoptosis in colorectal carcinoma cells treated with 4-hydroxy-2-nonenal and structurally related aldehydic products of lipid peroxidation. Chem Res Toxicol 2004;17:453–62.
41. Tang DG, La E, Kern J, Kehrer JP. Fatty acid oxidation and signaling in apoptosis. Biol Chem 2002;383:425–42.
42. Fruwirth GO, Hermetter A. Mediation of apoptosis by oxidized phospholipids. Subcell Biochem 2008;49:351–67.
43. Dupertuis YM, Meguid MM, Pichard C. Colon cancer therapy: new perspectives of nutritional manipulations using polyunsaturated fatty acids. Curr Opin Clin Nutr Metab Care 2007;10:427–32.
44. Stillwell W, Wassall SR. Docosahexaenoic acid: membrane properties of a unique fatty acid. Chem Phys Lipids 2003;126:1–27.
45. Davies CL, Loizidou M, Cooper AJ, Taylor I. Effect of γ-linolenic acid on cellular uptake of structurally related anthracyclines in human drug sensitive and multidrug resistant bladder and breast cancer cell lines. Eur J Cancer 1999;35:1534–40.